Egypt. J. Chem. **Vol. 64,** No. 3 pp. 1187 - 1195 (2021)

Egyptian Journal of Chemistry

http://ejchem.journals.ekb.eg/

Computational DFT Study of Gold Containing PVP/PEO/Gold Organometallic Polymer Nanocomposites

Amr M. Abdelghany;[a,*], Mortada I. Youssif;[b], Elmetwally M. Abdelrazek,[c,d], Dina S. Rashad,[e]

[a]*Spectroscopy Department, Physics Division, National Research Centre, 33 El-Behouth st., 12311, Giza, Egypt.*
[b]*Physics Department, Faculty of Science, Damietta University, P.O. Box 34517, New Damietta, Egypt.*
[c]*Physics Department, Faculty of Science, Al-Ula, Taibah University, Madina, Saudi Arabia.*
[d]*Physics Department, Faculty of Science, Mansoura University, 35516, Mansoura, Egypt.*
[e]*Dakahlia Roads and Transport Directorate, Suez Canal St., Mansoura, Egypt*

Abstract
Polyethylene oxide (PEO) and polyvinyl pyrrolidone (PVP) were used to prepare virgin and equimass fraction blend samples via an ordinary solution casting route. Polyblend was filled with a different mass fraction of green biosynthesized metallic gold nanoparticles (AuNP's). The organometallic Nanocomposites were then studied using different characterization techniques. X-ray diffraction (XRD) investigation supports the formation of a face-centered cubic (FCC) structure of AuNP's. FTIR spectral data reveals the persistence of the main vibrational groups in the polymeric matrix and suggests that the complexation process occurs via the carbonyl group. UV/Vis. is measurement used to estimate values of the optical energy gap and confirms the formation of AuNP's in the nano-scale through observation of the surface plasmon resonance (SPR) peak at about 562 nm. Density functional theory (DFT) studies were employed to confirm the suggested mechanism of complexation between constituting polymers and to retrace structural changes within the polymeric matrices. Zeta sizer and transmission electron microscopy (TEM) reveals that AuNP's were polydispersed with sizes ranging from 5-23.1 nm.

Keywords: PEO; PVP; AuNP's; DFT; FTIR; UV-Vis; TEM.

1. Introduction

PEO represents a class of polymeric materials with interesting properties resulting from its high chemical and thermal stability because it contains both amorphous and crystalline phases (semi-crystalline polymer). PEO polymer gains their importance from their ability to solvate a wide range of salts even at very high concentrations [1]. PVP is stable with reasonable electrical conductivity due to the charge transport mechanism. PVP has readily formed films with good wetting characteristics which makes it excellent coating or additive to coatings [2] in addition to its low cytotoxicity which makes them usually used in medicine, drug-control technology [3], and electrochemical based devices including batteries and liquid displays [4].

During the last decades, polymer blends and their combination with inorganic or organic fillers including transition metals and nanomaterials play a key role in the manufacturing of new materials suitable for different industrial and medical applications [1-4].

Green biosynthesis technique has gained special attention because they are environmentally friendly and benign. Plants used in biosynthesis are generally inexpensive, available, and nontoxic. AuNP's have attracted much more attention because of their biocompatibility and high prospective for use in medicine, and biology [5, 6], absorption, and strong scattering [6], tunable SPR [7, 8], and low toxicity [9, 10].

Chenopodium murale (C. murale) represents a species of plant annual fast-growing herb belonging to the Amaranthaceae family widespread worldwide

*Corresponding author e-mail: a.m_abdelghany@yahoo.com.; (Amr M. Abdelghany).
Receive Date: 30 December 2020, Accept Date: 15 January 2021
DOI: 10.21608/EJCHEM.2021.55871.3187

mostly in tropical and subtropical regions of Europe and North Africa [11]. C. murale leaf extract has been assumed to be a capping and reducing agent for the biosynthesis process of AuNP's which could be assumed green method and owes more advantages other synthesis routes including microbial synthesis route as the elaborated practice of culturing and preserving the cells is not required [12].

The present work aims to introduce, for the first time, a theoretical model (DFT) that describe a possible suggested method of interactions between Polyethylene oxide (PEO) and polyvinyl pyrrolidone (PVP) polymeric matrices and that containing biosynthesized Gold nanoparticles (AuNP's) combined with experimental spectroscopic tools including (FTIR) and UV/visible spectroscopy that confirm using DFT approach.

2. Experimental work

2.1. Materials

Polyvinyl pyrrolidone (PVP) off-white powder having a molecular weight of about 72000 g/mol supplied by SISCO Research Labs (India) and Polyethylene oxide (PEO) powder of molecular weight 40000 g/mol supplied by ACROS chemicals (USA) were used as received. High purity Tetrachloroauric (III) acid trihydrate 99.5% supplied by Merck, (Germany) was used for nanoparticle synthesis. C. murale plant leaves were collected from Mansoura district, Egypt.

Polymer blend thin film was prepared by a traditional solution casting technique. Equal mass fractions of both PEO and PVP dissolved in double distilled water under vigorous stirring at room temperature until a viscous dissolved solution was formed. A successively calculated amount of gold nanoparticles was added to the obtained viscous solution vigorously stirred at room temperature for about 2h to obtain a homogeneous bubble-free mixture. Viscous solutions were then casted onto polypropylene Petri-dishes and dried in an oven regulated at 50 °C for two days. Dried composite films peeled from the dishes and kept in dry media until use. The sample composition and nomination were listed in table (1). X-ray diffraction scans were performed with PANalytical X`Pert PRO machine using CuKα radiation (operating voltage 30kV, λ = 1.540 Å, within Bragg's angle (2θ) 10-70◦). FTIR optical absorption spectra recorded using a single beam spectrometer (Nicolet iS10) within the spectral range 4000–400 cm-1 while UV/Vis. spectra data collected using Jasco V570 double beam spectrophotometer in the wavelength range from 190 to 900 nm. Shape, size, distribution, and surface morphology were tested using TEM (JEOL-JEM-1011, Japan). Zeta potential measurements were performed for an aqueous solution of AuNP's using a zeta seizer nano-ZS (Malvern instruments, Ltd). Finally, the elemental analysis of biosynthesized gold nanoparticles was executed via atomic absorption spectrometry (AAS) using Perkin Elmer Analyst 800, USA.

Table 1. Sample composition and nominations

Sample	PEO	PVP	AuNP's
	Wt%		ml add × 450 ppm
PEO	100	0	0
PVP	0	100	0
Au0	50	50	0
Au1	50	50	1
Au2	50	50	2
Au4	50	50	4
Au8	50	50	8

2.2. Synthesis of C. murale plant extract and biosynthesis of AuNP's

C. murale plant leaf extract was prepared using distilled water. 25g of exhaustively washed plant leaf placed in a 500 ml Erlenmeyer flask with 100 ml distilled water. The flask was heated until boiling. The obtained solution was left to boil for about 1hr. The obtained extract was freeze-dried and filtered with Whatman filter paper as previously discussed [11]. A Stoppered Erlenmeyer flask was used for the preparation of 100 ml (5 mM auric chloride aqueous solution). 2 ml of prepared extract was added to the flask at room temperature and the pH value was adjusted at 10 using 0.1 M HCl and 0.1 M NaOH until pinkish-red color characterize the AuNP's was observed. The obtained solution was kept in dark until use [13].

2.3. Density Functional Theory calculations and models

The proposed calculation was performed using DMOL3 [14] program within the Materials Studio package [15]. DFT semi-core pseudopods calculations (dspp) were achieved via double numerical basis sets combined with polarization functional (DNP). These calculations are analogous in quality to that of 6-31G Gaussian basis sets [16]. Delley et al. exhibited that such calculation basis sets are more precise than that of the Gaussian basis of the same size [16]. The revised version of Perdew, Burke, and Ernzerh (RPBE) can be considered as the best exchange-correlation functional based on the generalized gradient approximation (GGA) [17, 18] that take account of the exchange and correlation effects of electrons. The geometry optimization is accomplished without any symmetry constraint for the studied polymer blend. Each fixed point has been designated by harmonic frequency calculations at the

same level of theory (RPEP/DNP) and then we specify the FTIR active harmonic frequencies.

3. Results and Discussions

3.1. Fourier transform infrared analysis FT-IR

FT-IR optical absorbance spectra were employed to estimate the structural groups present in virgin polymers (PEO and PVP) along with that of equal-mass blend and to study the interaction between both polymers as shown in Figure (1). Figure (1) illustrates FTIR spectral data of both virgin polymers, PEO and PVP, and their blend recorded within the range 4000-400 cm^{-1} at ambient room temperature.

Obtained data reveals the perseverance of the main vibrational bands that characterize studied virgin polymers in their position [19-26]. The assignment of observed vibrational bands and their position are listed in table 2.

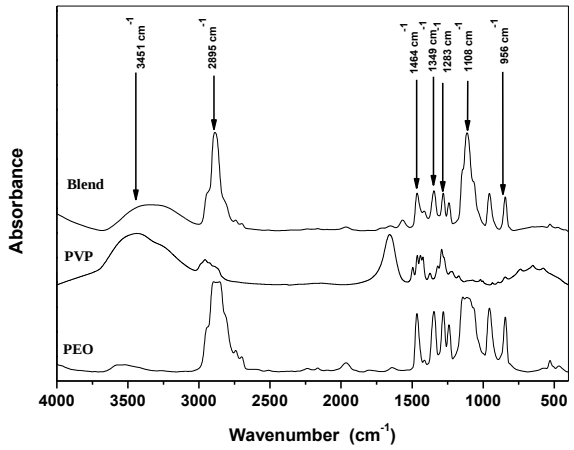

Fig. 1. FT-IR spectra of a pure blend, a pure PEO, and pure PVP.

Table 2. Observed band position and their position of virgin samples and their blend

Wavenumber (cm^{-1})	Band assignment	Reference
3451	OH stretching	19
2895	CH2 asymmetric stretching	20
1655	C=O symmetric stretching	21, 22, 23, 24
1446	CH2 scissoring vibrations	22, 23
1291	C–N symmetric stretching	26

The spectral data of studied samples reveal the presence of main characteristic bands of virgin samples at 3451, 2895, 1655, 1446, and 1291 cm^{-1} corresponding to stretching vibration of a hydroxyl group (OH)[19], CH_2 asymmetric stretching vibration [20], C=O stretching [21-24], CH_2 scissoring vibrations, C–N stretching of PVP [26] respectively. It is distinguished that, the double bond segments in the structure of studied materials may be considered as appropriate sites for polarons and/or bipolarons [25].

Moreover, the spectra of the blend sample exhibited a shift in some bands and/or a variation in the intensity of other bands that can be assumed to result from a significant interaction between the polymer blend. It was observed that the intensity of the stretching vibration attributed to a hydroxyl group (OH) decreases indicating a decrease in swelling properties with increasing PEO content. The spectra showed a new band at about 1570 cm^{-1} attributed to the possible interaction between the two polymers. Also, it was pragmatic that the intensity of the absorption band at about 2895 cm^{-1} (CH_2 asymmetric stretching) and about 1108 cm^{-1} (C-O-C stretching) increase with increasing PEO content.

The intensities of the characteristic bands of PEO at around 1464 cm^{-1}, 1349 cm^{-1}, and 1283 cm^{-1} (represented CH_2 scissoring, CH_2 asymmetric bending, and CH_2 asymmetric twisting respectively) decrease with increasing PVP content, also the intensity of the vibrational band at about 1655 cm^{-1} (C=O stretching) decrease after addition PEO content. Figure. 2 reveals FT-IR experimental absorption spectra of pure polymer blend and other samples with the same composition containing different concentrations of added AuNP's.

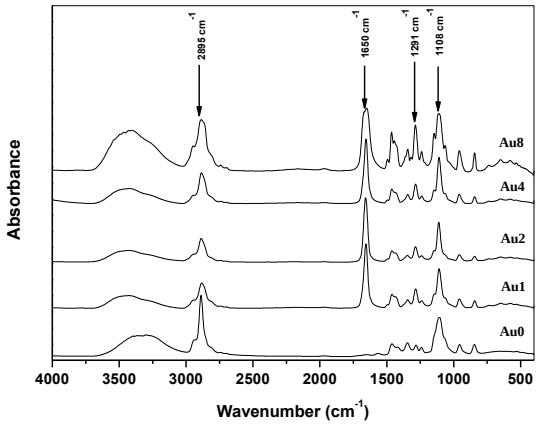

Fig. 2. FT-IR spectra of pure blend and biosynthesized gold NPs

The figure showed that the intensity of the vibrational band at about 2895 cm^{-1} (CH_2 asymmetric stretching) decreases in the case of small concentrations of Au (Au1, Au2) and increases at high concentrations of Au (Au4, Au8); this related to the crystallinity of XRD result.

The spectra also showed a new band at 1650 cm^{-1} which demonstrates the complexation between the Au nanoparticles and (PEO/PVP) polymer blend. A broad peak with two shoulders at about 1108 cm-1 (C-O-C stretching) becomes sharper with increasing the content of Au nanoparticles and the intensity of the vibrational band at about 1291 cm^{-1} (C–N stretching) increases with increasing Au nanoparticles content.

3.2. Density Functional Theory

Density Functional Theory is employed to be a measure of agreement between the theoretical and experimental data for the complex interaction of (PVP/PEO) poly blend and then doped with the biosynthesized AuNP's. There are four different probabilities of interaction between (PVP/PEO) poly blend shown in Fig. 3; Also Fig.4. Illustrates the optimized structure results of the four possible interactions with the obtained experimental and theoretical FTIR obtained from the optimized structure of possible modes of interaction respectively.

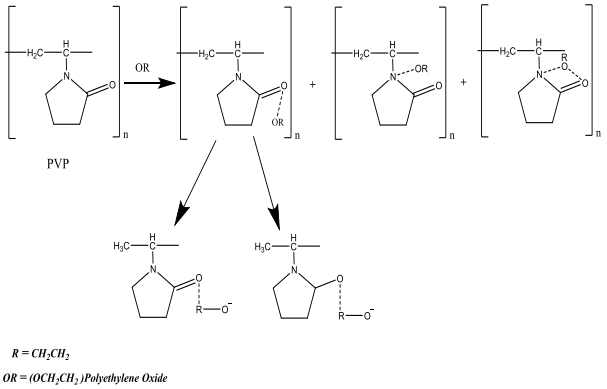

Fig 3. Mechanism of four possible interaction modes between PEO and PVP monomer.

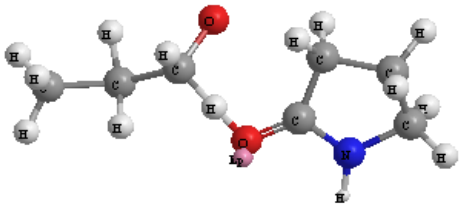

(a)

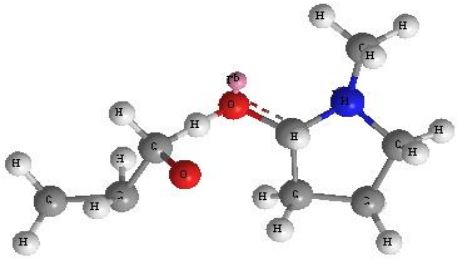

(b)

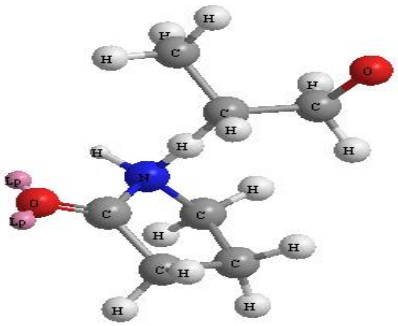

(c)

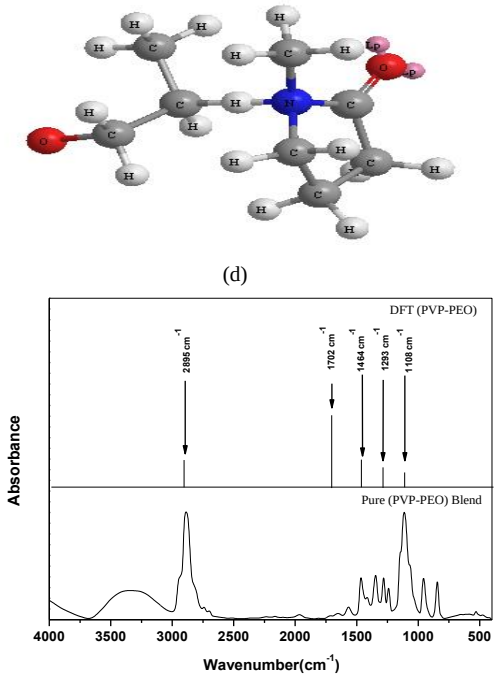

Fig. 4. Optimized structure of four possible interaction modes of PEO with PVP monomer with experimental and theoretical FTIR absorption spectra.

Theoretical calculations illustrate that shows that the new band obtained in the experimental data is not observed in its theoretical analogs and this may be attributed to shifting of the vibrational band (C=O stretching) from about 1655 cm-1 to 1702 cm^{-1}. These calculations show that the PEO and/or gold nanoparticles were stabilized with the oxygen atoms of pyrrolidone ring by chemical interaction, while other suggested mechanism of complexation between constituting polymers is not compatible with the experimental data [27-29].

For PEO/PVP/AuNP's; there are two possible probabilities of interaction between PVP/PEO polymer blend and AuNP's as shown in figure 5.

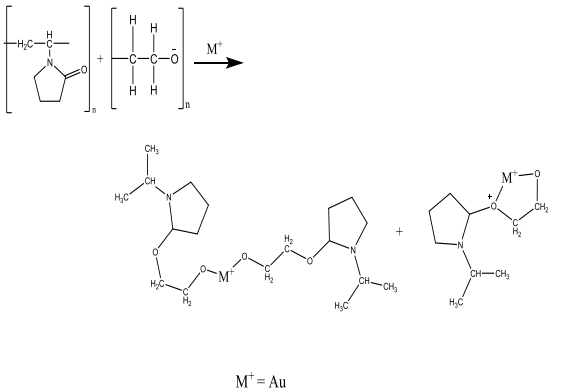

Fig. 5. Possible modes of interaction between PEO and PVP monomer with Au.

The two possible interactions may occur via the coordination between Au and two monomers of ether oxygen atoms in PEO or coordination via both the oxygen atom of carbonyl groups of PVP and ether oxygen atoms in PEO.

Figure 6. shows the optimized structure of two possible modes of interactions between PVP/PEO polymer blend and AuNP's with obtained theoretical and experimental FTIR obtained from the optimized structure of possible modes of interaction respectively.

A combination between theoretical calculation and experimental FTIR shows that there is a good agreement between theoretical calculation and experimental data and the more dominant interaction that occurs is the coordination of the AuNP's with the two monomers of ether oxygen atoms in PEO; while other suggested mode of interactions is rejected.

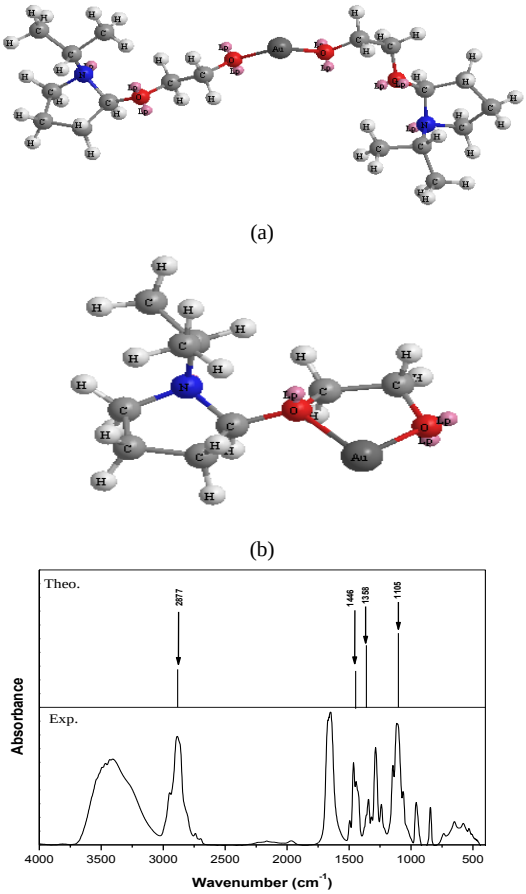

Fig. 6. Optimized structure of two possible interaction modes of PEO and PVP monomer with Au with experimental and theoretical FTIR absorption spectra

3.3. X-ray diffraction (XRD):

X-ray diffraction studies have been carried out to realize the semi- crystalline nature of the (PEO/PVP) blend and possible changes that occur in the semi- crystalline nature due to the addition of Au nanoparticles.

Figure 7. represents the X-ray diffraction of pure (PEO/PVP) polymer blend with different adding of Au nanoparticles. There are three crystalline peaks of PEO showed in pure (PEO/PVP) blend film, a peak of maximum intensity at 2θ ≈19.1˚, next maximum peak at 2θ ≈ 23.3˚ and there is a less intense peak at 2θ ≈26.7˚ [30]. The diffraction lines centered at 38.2º, 45.2º, and 64.6º corresponding to (111), (200), and (220) planes respectively of Au compound with face-centered cubic (FCC) of Au structure according to (JCPDS card no. 00-004-0784) [31].

However, on the addition of Au nanoparticles to the polymer blend, the intensity of these peaks increases gradually in case of a small concentration of Au (Au1, Au2). This indicates that the distribution of Au in the polymeric matrix becomes uniform and the structure is more organized, hence the Au play an effective role in the enhancement of the structure while in case of high concentration of Au (Au4, Au8) the intensity of these peaks decreases and the Au takes interstitial position. This result shows a marked decrease in the degree of crystallinity and an increase in the amorphous regions within the polymer blend matrix.

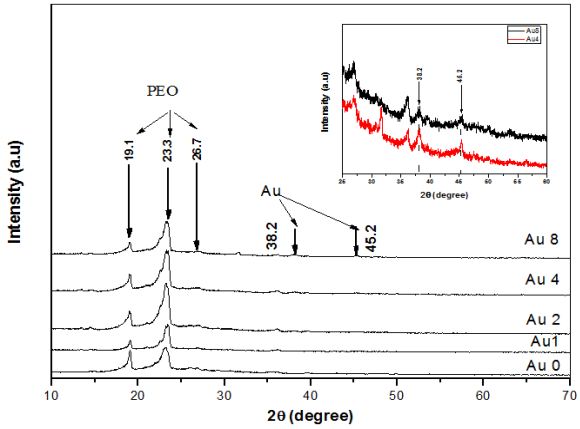

Fig. 7. X-ray diffraction pattern of pure (PEO/PVP) polymer blend with Au nanoparticles. In the inset, the diffraction lines around 38.2º and 45.2º characterizing Au- nanoparticles are shown on an enlarged scale.

Figure 8. represents the X-ray diffraction of pure Au nanoparticles; it is obvious that a peak at about 2θ ≈ 38.2º and 2θ ≈ 45.2º which belongs to pure Au nanoparticles appearing in the spectra of prepared samples.

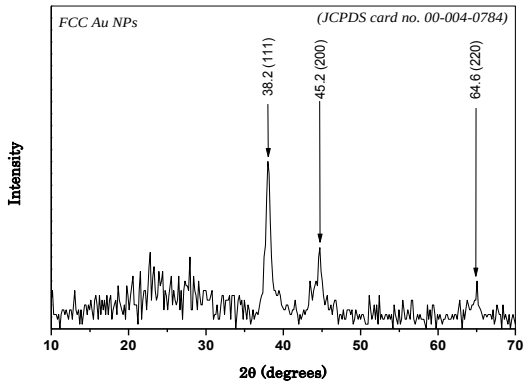

Fig. 8. X-ray diffraction pattern of pure Au nanoparticles. Numbers in bracket mark the Miller indices of the corresponding crystallographic planes according to JCPDS card no. 00-004-0784.

3.4. Ultraviolet and visible analysis UV/Vis.:

Figure 9 shows the UV/Vis. optical absorption spectral data of the studied pure samples and their blend containing gradual increasing content of AuNP's. A strong sharp charge transfer absorption at about 229 nm with the fundamental absorption edge attributed to π → π* transition within the carbonyl groups (C=O) was observed [32]. The absorption bands at about 232-234 nm in the spectra of gold modified samples combined with a small hump around 562 nm (inset figure) ascribed in terms of AuNP's addition and Surface Plasmon Resonance (SPR) of gold nanoparticles. The spontaneous formation of Au nanoparticles can be attributed to the direct redox between PVP and Au. The formation of AuNP's by C. murale leaf extract may be associated with the appearance of this band. The absorption edge is shifted to a longer wavelength as Au continents increase. Such changes may approve the complexation process between an organic matrix and an inorganic filler.

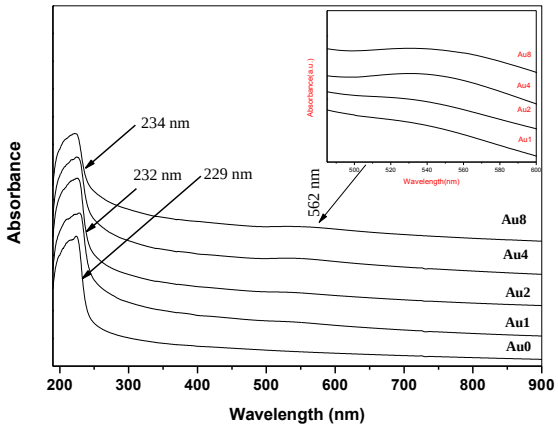

Fig. 9. UV/Vis. spectra of pure (PEO/ PVP) polymer blend doped Au nanoparticles. In the inset, the small hump at around 562 nm characterizing the SPR criteria of free electrons in the conduction bands of AuNP's.

The interpretation of such behavior may be correlated with the band structure of materials. The optical band gap energy can be expressed in terms of the wavelength at the absorption edge using the traditional equation ($E_g = hc/\lambda$) where h is Planck's constant and c is the velocity of light. Absorption coefficient (α), also correlated with sample absorbance (A) and thickness (d) as: $\alpha = 2.303\ A/d$. The optical energy gap (E_g) of amorphous materials associated with photon energy discussed in terms of direct electronic transition when (n=1/2) or direct electron transition when (n=2) in the following equations [33]:

$(\alpha h\nu) = \beta\ (h\nu - Eg)^{1/2}$ indirect (1)

$(\alpha h\nu) = \beta\ (h\nu - Eg)^{2}$ direct. (2)

Where β is a constant.

Davis and Shilliday [34, 35] illustrated that the occurrence of the near fundamental band edge, both direct and indirect transitions can be observed via what is called Tauc's plot shown in Figure 10, 11.

The value of the optical energy gap resulted from both methods is listed in table 2. From this table, it is clear that the values of the optical energy gap are increased with increasing Au nanoparticles content (Au1, Au2) as compared with that of pure blend indicating that the structure is more organized.

Further increase of gold (Au4, Au8) the values of these energies are decreased with increasing Au nanoparticles. The formation of chemical bonding between the chains of PEO/PVP blend and AuNP's is confirmed by decreasing the value of the optical energy gap which is the main reason for localized state generation. These results are supported by XRD studies.

Table 2. Absorption edge (λg) and optical energy gap [EgT and EgDM] for prepared samples.

Sample notation	Absorption edge (λg) (nm)	EgDM (eV)	EgT (eV)
Au0	248.76	4.583	5.14.98
Au1	260.42	4.352	5.04.76
Au2	255.10	4.521	5.14.86
Au4	259.74	4.203	5.04.77
Au8	262.47	4.150	5.04.72

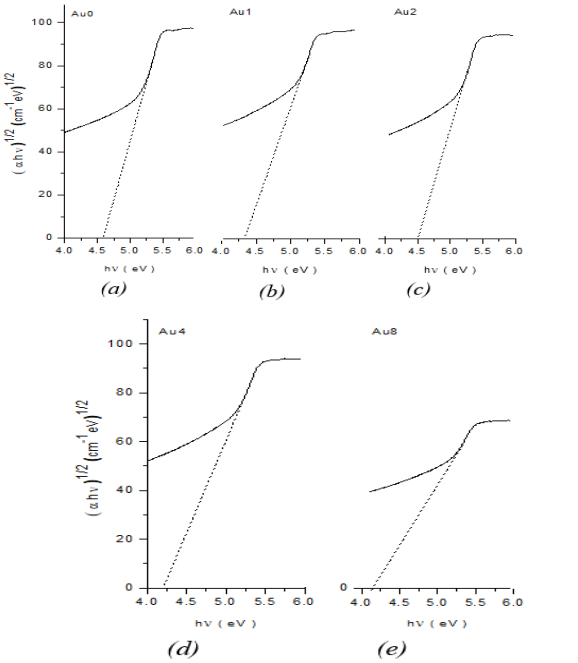

Fig. 10. $(\alpha h\nu)1/2$ versus photon energy for pure blend (PEO/PVP) polymer blend doped Au nanoparticles films.

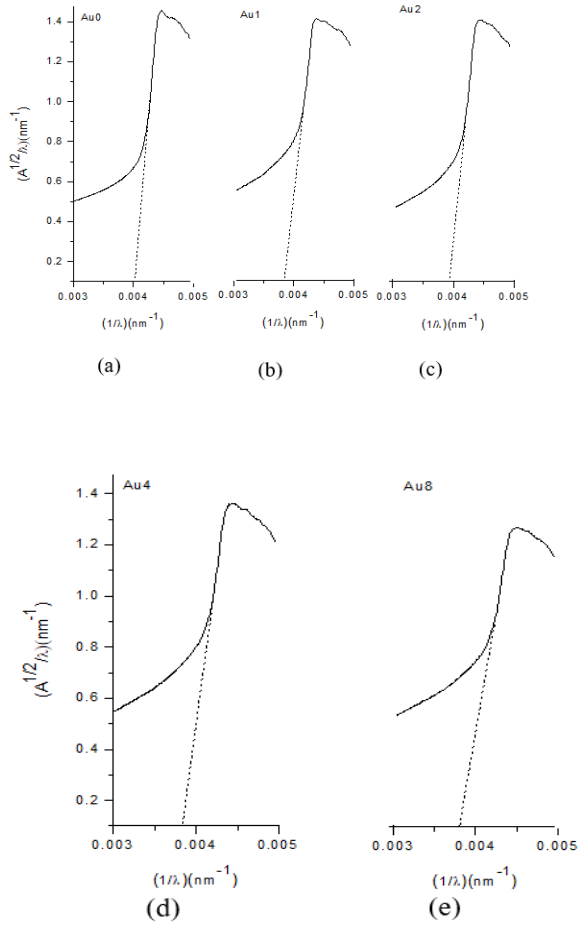

Fig. 11. $(A1/2/\lambda)$ versus $(1/\lambda)$ for pure blend (PEO/PVP) polymer blend doped Au nanoparticles films.

4.4. Transmission electron microscopy (TEM):

Figure 12. showed that the obtained AuNP's by C. murale leaf extract shows a non-uniform spherical shape and the average size of the distribution from 5-23.1 nm. For the zeta potential distribution study, peak number and peak area give an important explanation. Three peak cycles of different counts were run and the average of the counts was taken. The mean diameter of the particle is given by the peak meanwhile the percentage of mean diameter is given by the peak area according to the intensity and the size distribution by intensity is shown in Figure 13 (a, b) respectively.

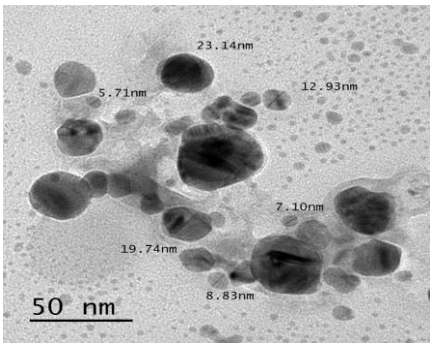

Fig. 12. Shows the TEM image of the AuNP's extracted from fresh leaves of C. murale.

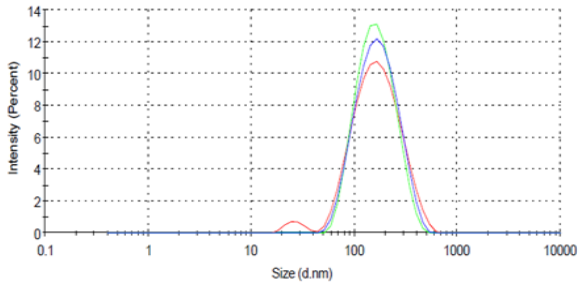

(a)

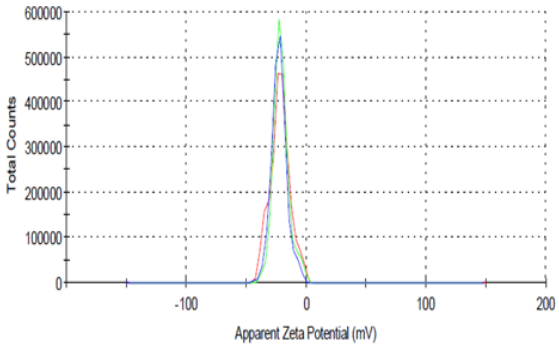

(b)

Fig. 13. (a) Zeta Size distribution, and (b) Zeta Potential of gold nanoparticles.

Conclusions

Samples of equi-mass PVP/PEO polymer blend containing biosynthesized Gold nanoparticles (AuNP's) were successfully synthesized and tested. XRD confirmed that prepared AuNP's was face-centered cubic (FCC) AuNP's with (111), (200), and (220) reflection planes. FTIR reveals the persistence of the main vibrational groups in the polymeric matrix and suggests that the complexation process occurs via the carbonyl group. The new band obtained in the experimental data and not observed in its theoretical analogies attributed to the shift (C=O stretching) from about 1655 cm-1 to 1702 cm-1. These calculations show that the PEO and/or AuNPs were stabilized with the oxygen atoms of pyrrolidone ring by chemical interaction, while other suggested mechanism of complexation between constituting polymers was forbidden as confirmed by DFT. Zeta sizer and transmission electron microscopy (TEM) reveals that AuNP's were polydispersed with sizes ranging from 5-23.1 nm.

References

[1] Kumar K. K., Ravi M., Pavani Y., Bhavani S., Sharma A. K., Narasimha Rao V. V. R., Investigations on the effect of complexation of NaF salt with polymer blend (PEO/PVP) electrolytes on ionic conductivity and optical energy band gaps, Physica B, 406, 1706 - 1712(2011).

[2] Tsutsumi N., Molecular design of photorefractive polymers, Polymer Journal, 48, 571-588(2016).

[3] Seabra A. B. and Oliveira M.G., Poly (vinyl alcohol) and poly (vinyl pyrrolidone) blended films for local niric oxide release, Biomaterial, 25, 3773- 3782(2004).

[4] Tsutsumi H., Doi H., Oishi T., Helical aggregate formation of cholate salts in poly (N-vinyl-2-pyrrolidinone) gel and its effect on conductivity enhancement, Journal of Power Sources, 68, 364 - 367(1997).

[5] Sperling R. A., Gil P. R., Zhang F., Zanella M., Parak W. J., Biological applications of gold nanoparticles, Chemical Society Reviews, 37, 1896 - 1908(2008).

[6] Jain P. K., Lee K. S., El-Sayed I. H., El-Sayed M. A., Calculated absorption and scattering properties of gold nanoparticles of different size, shape, and composition: applications in biological imaging and biomedicine, Journal of Physical Chemistry B. 110, 7238 - 7248(2006).

[7] Huang X. and El-Sayed M. A., Gold nanoparticles: Optical properties and implementations in cancer diagnosis and photothermal therapy, Journal of Advanced Research, 1, 13 – 28(2010).

[8] Narayanan K. B. and Sakthivel N., Phytosynthesis of gold nanoparticles using leaf

extract of Coleus amboinicus Lour, Materials Characterization, 61, 1232 - 1238(2010).

[9] Farea M.O., Abdelghany A.M., Oraby A. H., Optical and dielectric characteristics of polyethylene oxide/sodium alginate-modified gold nanocomposites. RSC Advances, 10, 37621-37630(2020).

[10] Boisselier E. and Astruc D., Gold nanoparticles in nanomedicine: preparations, imaging, diagnostics, therapies and toxicity, Chemical Society Reviews, 38, 1759 - 1782(2009).

[11] Abdelghany A. M., Abdelrazek E. M., Badr S. I., Abdel-Aziz M. S., Morsi M. A., Journal of Saudi Chemical Society, 21528-537,(2017).

[12] Youssif M.I., Abdelghany A.M., Abdelrazek E.M., Rashad D.S., Zidan H.M., Structure dielectric correlation of PEO/PVP incorporated with biosynthesized gold nanoparticles. Journal of Polymer Research, 27, 1-14(2020).

[13] Dwivedi A. D. and Gopal K., Biosynthesis of silver and gold nanoparticles using Chenopodium album leaf extract, Colloids and Surfaces A, 369, 27–33(2010).

[14] Wu X. and Ray AK., Density-functional study of water adsorption on the PuO_2 (110) surface, Physical Review B, 65, 85403(2002).

[15] Hehre W. J., Radom L., Schleyer P.V.R., Pople J.A., Ab Initio Molecular Orbital Theory, John Wiley, New York. (1986).

[16] Materials Studio, Accelrys software Inc., San Diego, USA. (2011).

[17] Hammer B., Hansen L. B., Nørskov J. K., Improved adsorption energetics within density-functional theory using revised Perdew-Burke-Ernzerhof functionals, Physical Review B 59 (1999) 7413.

[18] Ni J., Quintana M., Song S., Adsorption of small gas molecules on transition metal (Fe, Ni and Co, Cu) doped graphene: A systematic DFT study. Physica E: Low-dimensional Systems and Nanostructures, 1161, 13768(2020).

[19] Nobert M. B. (Ed.), "Encyclopedia of Polymer Science and Technology", 14, Wiley, New York, (1971).

[20] El-Gamal S., Elsayed M., Positron annihilation and electrical studies on the influence of loading magnesia nanoribbons on PVA-PVP blend. Polymer Testing, 89, 106681(2020).

[21] Laot C. M., Marand E., Oyama H. T., Spectroscopic characterization of molecular interdiffusion at a poly(vinyl pyrrolidone)/vinyl ester interface, Polymer , 40, 1095 -1108(1999).

[22] Lewandowska K., The miscibility of poly (vinyl alcohol)/poly (N-vinylpyrrolidone) blends investigated in dilute solutions and solids, European Polymer Journal, 41(2005) 55 - 64.

[23] Abdelaziz M. and Abdelrazek E. M., Effect of dopant mixture on structural, optical and electron spin resonance properties of polyvinyl alcohol, Physica B, 390, 1- 9(2007).

[24] Wu H. D., Wu I. D., Chang F.C., The interaction behavior of polymer electrolytes composed of poly (vinyl pyrrolidone) and lithium perchlorate (LiClO4), Polymer, 42, 555 - 652(2001).

[25] Tawansi A., El-Khodary A., Abdelnaby M. M., A study of the physical properties of $FeCl_3$ filled PVA, Current Applied Physics, 5, 572 - 578(2005).

[26] Kumar G. N. H., Rao J. L., Gopal N. O., Narasimulu K. V., Chakradhar R. P. S, Rajulu A.V., Spectroscopic investigations of Mn^{2+} ions doped polyvinylalcohol films, Polymer, 45, 5407 - 5415(2004).

[27] Abdelghany A. M., Abdelrazek E. M., Rashad D. S., Impact of in situ preparation of CdS filled PVP nano-composite, Spectrochimica Acta, Part A, 130, 302 - 308(2014).

[28] Abdelghany A. M., Mekhail M. Sh., Abdelrazek E. M., Aboud M.M., Combined DFT/ FTIR structural studies of monodispersed PVP/Gold and silver nano particles, Journal of Alloys and Compounds, 646, 326 - 332(2015).

[29] Abdelghany A. M., Mekhail M. Sh., Abdelrazek E. M., Aboud M.M., Spectroscopic inquest of CdS, PbS and ZnS Doped PVP composite: A Density Functional Theory Approach, Research Journal of Pharmaceutical, Biological and Chemical Sciences , 6, 1686 – 1697(2015).

[30] Mihaylova M. D., Krestev V. P., Kresteva M. N., Amzil A. and Berlinova I. V., Amphiphilic graft copolymers with poly (oxy ethylene) side chains: supermolecular structure in solid state: I. WAXS studies, European Polymer Journal , 37, 233 - 239(2001).

[31] State R., Papa F., Dobrescu G., Munteanu C., Atkinson I., Balint I., Volceanov A., green synthesis and characterization of gold nanoparticles obtained by a direct reduction method and their fractal dimension, Environmental Engineering and Management Journal, 14, 587 - 593(2015).

[32] Abdelrazek E. M., Spectroscopic studies on the effect of doping with $CoBr_2$ and $MgCl_2$ on some physical properties of polyvinylalcohol films, Physica B, 403, 2137 - 2142(2008).

[33] Thutupalli G. K. M. and Tomlin S. G., The optical properties of thin films of cadmium and zinc selenides and tellurides, Journal of Physics D, 9, 1639(1976).

[34] Davis P. W. and Shilliday T. S., Some Optical Properties of Cadmium Telluride, Physical Review 118, 1020(1960).

[35] Abouhaswa A.S., Rammah Y.S., Turky G.M., Characterization of zinc lead-borate glasses doped with Fe 3+ ions: optical, dielectric, and ac-conductivity investigations. Journal of Materials Science: Materials in Electronics, 31, 17044-17054(2020).